Clinics in Oncology

Research Article
Published: 16 May, 2023

Advances in Positron Emission Tomography for Proton Therapy Dose Monitoring

Rameshwar Prasad and Jagadeesh S Singh*

Department of Diagnostic Radiology and Nuclear Medicine, Rush University Medical Centre, USA

Abstract

Proton therapy is increasingly becoming a popular radiation therapy modality owing to its unique characteristics of Bragg peak. Proton therapy suffers from various uncertainties introduced during radiation treatment planning and dose delivery. PET imaging of proton induced positron emitter distributions provides *in-vivo* monitoring and verification of dose delivered in proton therapy. In this review physics principles, history, development, and applications of PET to monitor and verify radiation dose delivered in proton therapy are presented. Different configurations of in-room in-beam, in-room off-beam, and off-room PET with proton beam are discussed. Insights on future developments and applications of PET as proton dose monitoring and verifying are presented.

Keywords: Proton therapy; Positron emission tomography; Range; Dosimetry; Detector

Introduction

Radiation Therapy (RT) exploits the highly energetic radiation from photons or particles to irradiate the cancerous tissues that eventually damages the Deoxyribonucleic Acid (DNA) of cancer cells and stopping their ability to divide and proliferate. Several radiation therapy techniques exist such as external beam therapy using photons or charged particles; and brachytherapy in which the radiation is implanted inside the body for irradiation. Molecular radiopharmaceutical therapy treats the malignancy by injecting or infusing subjects with a combined radioisotope and a suitable biochemical carrier. On the treatment path and beyond, the radiation may also damage the non-target healthy tissues. Proton therapy is increasingly becoming a popular radiation therapy modality due to its unique physical characteristic 'Bragg Peak' of depositing the radiation dose to a limited depth without any downstream exit dose [1]. This unique characteristic of proton beam therapy delivers the maximum radiation dose to the target and minimum to the non-target resulting in less toxicity, complications, and side effects [2]. Monoenergetic proton Bragg peak can target narrow depth ranges in the treating subjects. To treat entire tumor or larger distribution Bragg peak beam is spread-out laterally called Spread-Out Bragg Peak (SOBP). To achieve SOBP, energy of the incident proton beam is varied, and various energies are modulated to spread the peak for flat dose distribution [3] as shown in Figure 1.

Although proton therapy is effective and widely recognized for cancer treatment it is affected from many uncertainties such as the dose deposition distribution, treatment volume motion, proton range, Stopping-Power-Ratio (SPR) estimation, and others [4-7]. The sharp fall-off of dose deposition curve at the Bragg peak region lead to more uncertainties in proton therapy treatment planning than in case of exponential fall-off in photon therapy. Uncertainties in proton therapy can also lead the treatment area not fully treated (underdosing) or deposit dose to downstream healthy areas causing overdosing of treatment area [8]. Measurement of these uncertainties is crucial to fully exploit the advantages of proton beam therapy for cancer treatment.

Positron Emission Tomography (PET), an *in-vivo* and non-invasive positron detector and imager, is promising modality to monitor and verify the range and the dose deposited in the patient during the proton therapy [9-12]. The concept behind using PET for proton therapy dosimetry and therapy monitoring is that during proton irradiation, when proton interacts the elements in the tissues, positrons emitters are produced by photonuclear reactions. Table 1 lists the useful and relevant positron emitter produced in tissue during proton beam therapy. Although small quantities and short-lived positron emitters are produced, these can be detected and used for dosimetry with advanced and state-of-art instrumentation and signal processing in PET [13]. PET imaging and data can be acquired either during the proton beam irradiation (in-beam) [14-17] or after the irradiation (in-room/ off-room) [18-21].

Correspondence:
Rameshwar Prasad, Department of Diagnostic Radiology and Nuclear Medicine, Rush University Medical Centre, 1653 W. Congress Parkway, Chicago, IL 60612, USA, Tel: +1 312 947 0309; Fax: +1 312-942-7244; E-mail: rameshwar_prasad@rush.edu

Received Date: *28 Apr 2023*
Accepted Date: *11 May 2023*
Published Date: *16 May 2023*

Citation:
Prasad R, Singh JS. Advances in Positron Emission Tomography for Proton Therapy Dose Monitoring. Clin Oncol. 2023; 8: 2001.

ISSN: 2474-1663

PET-based proton therapy monitoring of the dose delivery provides comparison between measured β+ -activity distribution from the planned dose distribution. This compared information can check the uncertainties in the delivered dose caused by patient mispositioning and anatomical alterations of irradiated tissue. This paper reviews the principles, history, developments and application of PET for radiation dose and range verification in proton beam therapy.

Material and Methods

PET principle

PET imaging involves the coincidence detection of two 511-kiloelectron Volt (keV) annihilation photons generated as a by-product of positron decaying nuclei such as produced during the proton therapy. The basic underlying principle of PET detection is shown in Figure 2. These annihilation photons are detected using dedicated PET scanners by means of scintillation detectors arranged in geometric shapes such as ring in 2-dimensional, 3-dimesional, or two opposing arc that surrounds the patients [22]. Fundamentally, PET system is a scintillation detector with counting and 3D imaging capabilities. Scintillation crystal is one of the vital components of PET scanners. The ideal characteristics of scintillation crystals are high light yield, fast rise and decay times, high stopping power and good energy resolution, linearity of response with energy, low cost, availability, moisture resistance, and ductility. Some of the commonly used scintillation detectors for PET imaging are Bismuth Germanate (BGO), Lutetium Orthosilicate (LSO), Lutetium-Yttrium-Oxyorthosilicate (LYSO) and Lutetium-Gadolinium-Oxyorthosilicate (LGSO) [23]. The characteristics of various scintillation detectors for PET imaging are shown in Table 2.

The detection of two photons simultaneously within a short time interval (coincidence timing window) leads to a coincidence event, generated based on the energy deposited by the photon in the scintillating detectors. These events are termed as prompt events. However, the accidental detection of two photons from uncorrelated positron annihilations gives rise to random events. There is possibility that one or both of the photons from a single positron annihilation detected within the coincidence timing window may have undergone a Compton interaction. These events are deflected from their actual direction and are termed scattered events [23]. Different kind of coincident events are graphically shown in Figure 3. When two annihilation photons are detected simultaneously within a predefined coincidence timing window, it is assumed that a positron was emitted somewhere on the line that connects the two opposite detectors involved. The line connecting the two detectors is termed a Line-of-Response (LOR) [24]. PET data can be acquired either in 2-Dimensional (2D) mode or 3-Dimensional (3D) mode. The detected coincidence events are reconstructed to estimate the spatial distribution of positron emissions [25]. Annihilation localization is improved by using the time-of-flight information in the iterative reconstruction using equation (1).

$$\Delta d = (\Delta t * c)/2 \quad \ldots. (1)$$

Where, Δt is the difference in arrival times of photons. Δd represent the depth resolution.

PET instrumentation

PET instrumentation consists of scintillation detector which converts the incident photon to visible light; visible light to elections/current converter such as Photomultiplier Tube (PMT) or photodiodes; data acquisition and signal processing electronics; computational image formation and display.

Table 1: Useful positron emitter produced in tissue during proton beam therapy.

Reaction	Threshold energy (MeV)	Half-life (min)	Positron energy (MeV)
$^{16}O(p, pn)^{15}O$	16.79	2.037	1.72
$^{16}O(p, \alpha)^{13}N$	5.66	9.965	1.19
$^{14}N(p, pn)^{13}N$	11.44	9.965	1.19
$^{12}C(p, pn)^{11}C$	20.61	20.39	0.96
$^{14}N(p, \alpha)^{11}C$	3.22	20.39	0.96
$^{16}O(p, \alpha pn)^{11}C$	59.64	20.39	0.96

Scintillation detector

Atoms in the scintillating material gets excited or ionized when radiation interacts with them. These excited or ionized atoms release visible light when they deexcites or recombines to the ground state. Amount of energy deposited by impinging radiation is proportional to the amount of visible light energy released.

Scintillator crystals comes in various category of liquid or solid, organic or inorganic, and crystalline or non-crystalline. However, inorganic scintillators are commonly used in PET imaging due to their higher density and atomic number, leading to better detection efficiency (Table 2). In scintillator the valence (ground state) and conduction bands (excited state) are separated by a band gap of 5 eV or higher. A pure crystal, free of defects or impurities, would not have no electronic bands. To overcome this, most scintillators are doped with an activator ion that adds energy levels in the forbidden band gaps. Initial PET started with the use of thallium-doped Sodium Iodide (NaI[Tl]) scintillator crystal because of its known characteristics and performance for Anger gamma cameras. NaI(Tl) was discovered in 1948 by Hofstadter (8). After discovery of bismuth germanate ($Bi_4Ge_3O_{12}$ or BGO) scintillator in 1970s, a high density and with better gamma ray detection efficiency, it became choice of PET scintillator due to its higher detection efficiency than NaI(Tl). Nowadays, cerium-doped Gadolinium Oxyorthosilicate (Gd_2SiO_5[Ce] or GSO) and cerium-doped Lutetium Oxyorthosilicate (Lu_2Si0_5[Ce] or LSO) are commonly used due to their fast light output and quick response time to the incident radiation [26].

Different rectangular dimensions of scintillator crystal, for example 0.5 mm × 0.5 mm × 20 mm of LSO crystals, are used in PET depending on the desired goal of higher sensitivity and or higher spatial resolution.

Photodetector and electronics

Photodetector is a crucial component in the PET detection process. Photomultiplier Tube (PMT) is robust and reliable photodetector and electron amplification device which has been consistently used in scintillator-based radiation detection. PMT consist of photocathode which covert visible light to electrons and various dynodes to amplify the elections for signal detection and processing. Traditional PMTs provides with optimized design and multiple dynodes can achieve signal gain factor of 10^6 [27]. Multi-channel PMTs are optically coupled to the PET scintillator crystals in various designs such as, quadrant-sharing in which 2D array of crystals coupled to 4 PMTs [28], or an array of crystals coupled to a multi-channel PMT [29].

Traditional PMTs are now being replaced by Silicon

Table 2: Characteristic of scintillation crystals used in current PET scanners.

Scintillator	BGO	LSO	GSO	LGSO	LYSO
Chemical formula	$Bi_4Ge_3O_{12}$	Lu_2SiO_5:Ce	Gd_2SiO_5:Ce	$LuGdSiO_5$:Ce	$LuYSiO_5$:Ce
Density (g/cc)	7.13	7.4	6.71	5.3	7.19
Effective Z	75	66	60	61-65	60
Principal decay time (ns)	300	42	60	40	40
Peak wavelength (nm)	480	420	440	420	420
Refractive Index	2.15	1.82	1.95	1.8	1.81
Light Output (PMT) *	15	75	20	38	75
Light Output (APD) *	30	85	40	55	85
Attenuation length (mm)$	10.4	11.5	14.2	11.6	11.2
Hygroscopic	No	No	No	No	No

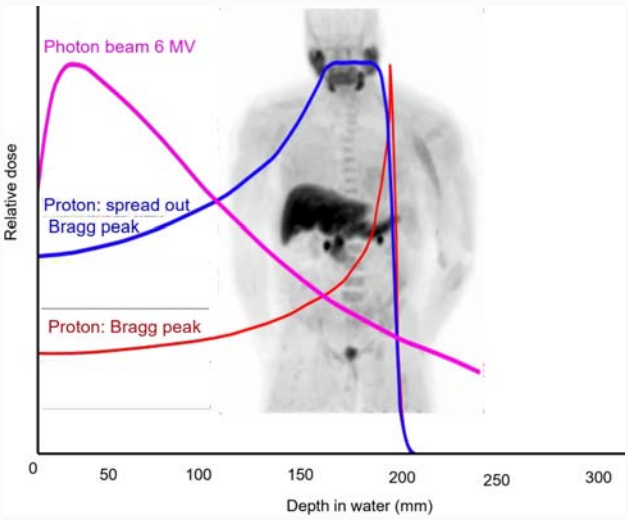

Figure 1: Relative dose distribution in tissues for 6 MV photons, proton Bragg peak and its spread for treatment volume.

Photomultipliers (SiPMs) which provides excellent timing resolution below 1 ns, and ~106 intrinsic gain equivalent to that of PMTs, and compatible with the magnetic field [30]. SiPM is a semiconductor unit consist of Avalanche Photodiode (APD) segments attached in parallel. The APDs are works in Geiger Mode, in which the bias voltage applied is greater than the reverse breakdown voltage producing a large internal electric field. An incident photon produced a carrier into this electric field resulting a large pulse of signal that can be further analyzed by processing circuits [31] Figure 4 shows the advances in photon detection using conventional PMTs to semiconductor silicon PMTs and APDs.

The positional and energy signal from the PET detector is fed to the multichannel analyzer to accept the desired energy range. The pulses from the PMTs are also passed through a differential discriminator to sort them according to pulse height. Usually there is a Lower Energy-Level Discriminator (LLD), and an Upper Energy-Level Discriminator (ULD) which may be used to reject pulses below or above particular values. The LLD can be used to discriminate against scatter, as scattered annihilation photons have lower energy than those which are unscattered. Each pulse is passed to coincidence circuitry for true signal processing [32]. Iterative reconstruction techniques with image formation and degradation models are used to reconstruct the list mode data to images.

PET for proton therapy dosimetry and monitoring

The first use of PET for *in-vivo* monitoring of radiation therapy is reported in 1988 by Llacer at Lawrence Berkeley National Laboratory [33]. However, first clinical use of PET for monitoring of radiotherapy was shown in 1997 at the experimental carbon ion therapy facility at GSI Center for heavy ions research, Darmstadt, Germany [34].

PET data for proton therapy dosimetry and monitoring can be acquired in three configurations. 1. In-room on-beam PET: PET imaging is integrated to proton therapy and acquire data during irradiation. 2. In-room off-beam PET: PET imaging data are

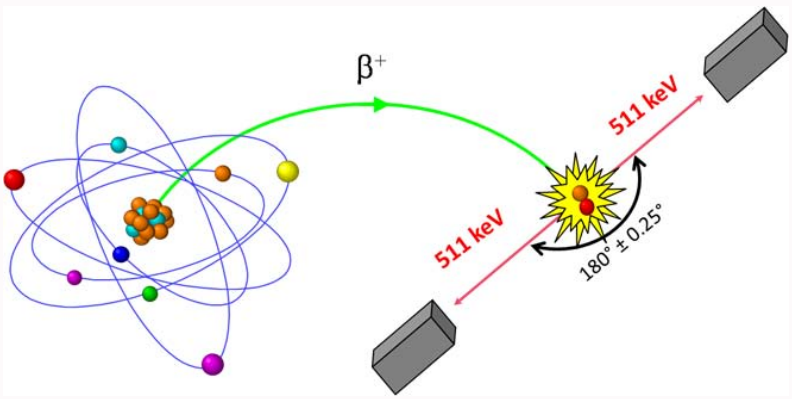

Figure 2: Representation of positron emission and annihilation processes and coincidence detection of resulting annihilation photons emitted back-to-back, each having energy of 511 keV.

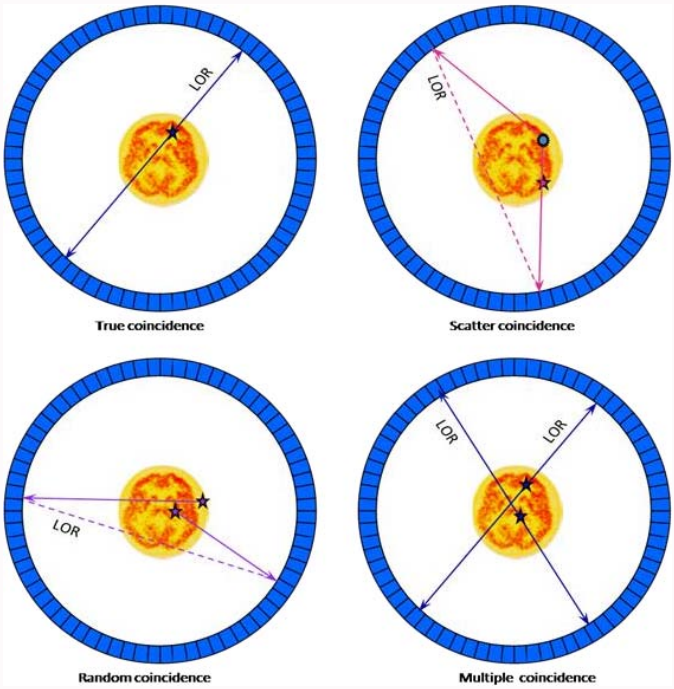

Figure 3: Different types of coincident events in PET imaging shown on a single detector ring.

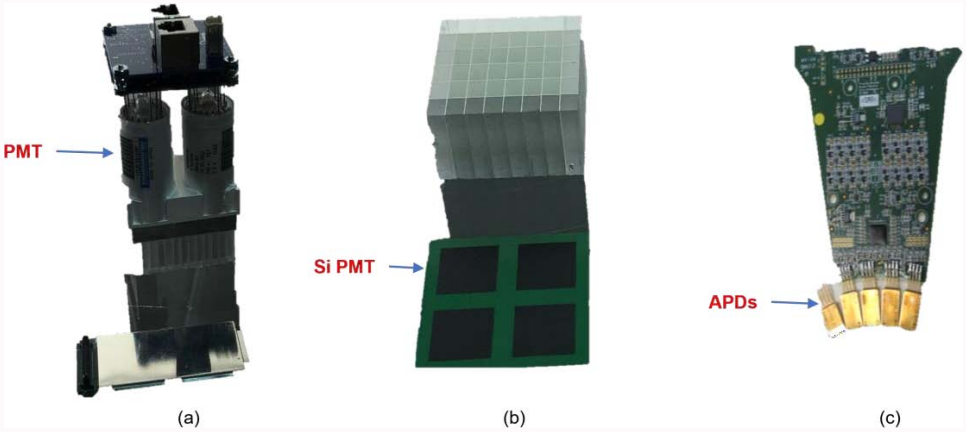

Figure 4: Advances in photo multiplier tubes (a) conventional PMTs (b) Silicon PMTs (c) APDs.

acquired sooner after the irradiation completion in the same room. 3. Off-room- PET: PET imaging acquisition is performed in outside the treatment room after irradiation completion. Figure 5 shows different configurations for PET based proton dose monitoring and verification.

In-room on-beam PET

In-room In-beam PET, the acquisition and detection of positron emitters is integrated and generally perform simultaneous with the proton therapy irradiation. In-room on-beam PET provides higher counting statistics (dose distribution) due to minimal biological and physical decay of positron emitters. Since the patient does not move between the beam irradiation and PET imaging repositioning and anatomical errors are reduced to zero or minimal. Several in-room on-beam PET detectors are currently in clinical applications around the world. Some of them are the Helmholtz Centre for Heavy Ion Research (GSI), Darmstadt, Germany [34], the Heavy Ion Medical Accelerator (HIMA) in Chiba, Japan [16]; the CATANA Proton therapy Center in Catana, Italy [35], and the National Cancer Center (NCC), Kashiwa, Japan [36].

Major challenge with in-room on-beam PET is the integration of PET hardware with the proton therapy gantry and nozzle. Full-ring PET scanners are not feasible with the beam and patient support hardware, hence partial ring or dual headed PET scanners are commonly integrated. Partial detectors provide lower signal detection that full ring [8]. However, with the time-of-flight and digital SiPMTs the PET signal is significantly improved [17,37]. Another challenge for in-room on-beam PET scanner is to avoid damage and activation of scintillator and hardware due to direct beam [38]. Computed Tomography (CT) based image corrections and improvements of PET imaging may add challenge, but this could be alleviated by use of daily cone-beam CT [39].

In-room off-beam PET

In-room off-beam PET involves use of uses a dedicated PET

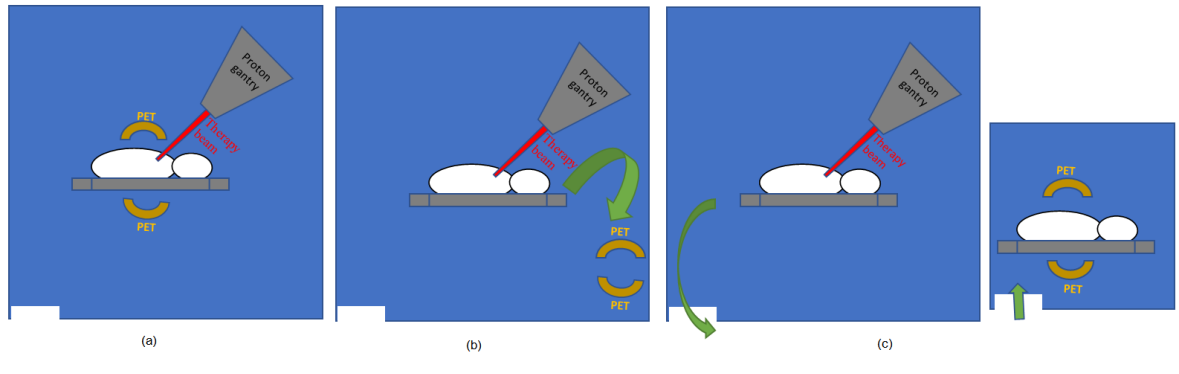

Figure 5: Different PET based Proton dose monitoring and verification (a) In-room on-beam (b) In-room off-beam (c) off-room.

scanner stationed within the treatment room for PET imaging. In-room off-beam PET is a trade-off between in-beam and off-line PET due to alleviation of integration challenge and associated costs. Since in-room PET does not acquire data simultaneous to therapy beam, geometric constraints does not pose problem. Any dedicated PET or PET/CT scanner with full-ring or partial ring can be used in the room. Francis H. Burr Proton Therapy Centre, MGH reported first in-room PET studies using in-room, mobile brain PET scanner, NeuroPET [40]. Decay and wash out of the positron emitters during the time to position in PET gantry reduces the PET counts than in-beam PET. Another challenge for in-room off-beam PET is the accurate co-registration of PET with the planning CT. However, this can be improved by using the combined PET/CT scanner [40].

Off-room PET

In off-room PET, PET images are acquired outside of the treatment room using a dedicated PET or PET/CT scanner. Time to PET acquisition post irradiation makes the positron radioactivity decay (short-lived) and washout that in-beam and in-room PET imaging. Hence off-room PET measures mostly long-lived ^{11}C as short lived ^{15}O usually decays by the time of PET imaging. Clinical use of off-line PET has shown its application for dose monitoring and range verification in proton therapy [19,41,42]. A study lead by Parodi K have shown that measured activity from the offline PET scan was compared to the expected activity distribution calculated using the FLUKA Monte Carlo code accounting for biological decay and image formation. They have shown that monitored range of proton depth was accurate to within 2 mm [18].

Future developments and applications

PET imaging is promising and has proven successful in *in-vivo* verification and monitoring of proton range and delivered dose for cancer treatment. However, it still has many challenges to overcome and become widely clinically accepted modality. PET imaging measures the β+ radioactivity arising from nuclear reactions between the ions of the beam and the nuclei of the tissue. The positron emitters produced have short life and are not abundant.

Future advancement such as time-of-flight incorporation and optimized semiconductor photodetector SiPMTs will increase the sensitivity of PET detection. Scintillators with high timing resolution of sub picoseconds will localize the events more accurately. 4D image reconstruction with attenuation, scatter and motion correction will further improve the PET image quality. Clinical applications development may include the kinetic tracer analysis of positron tracer wash out to provide the biological parameters of dose response and fractionation on-the-fly for more crucial dose targeting and monitoring. Newer dose delivery techniques such as spot beam scanning and Flash therapy will raise new challenges for the treatment verification with PET. It is foreseen that many current challenges in PET imaging for proton therapy will be addressed with widened applications.

Conclusion

A review of physics principles, history, development, and applications of PET to monitor and verify radiation dose delivered in proton therapy is presented. Proton therapy is a rapidly expanding cancer treatment that employs a proton beam to irradiate diseased tissue instead of photons. PET imaging has been proven to be a reliable and promising modality for *in-vivo* dose verification of proton beam therapy. PET provides correspondence between the measured dose distribution and treatment planned dose distribution. In-beam PET imaging for proton therapy is attractive, avoiding positrons physical and biological decay and providing immediate information about the dose delivery.

Acknowledgement

The author would like to thank Prof. Habib Zaidi, Geneva University for his guidance on PET instrumentation and physics.

References

1. Bragg WH, Kleeman R. XXXIX. On the α particles of radium, and their loss of range in passing through various atoms and molecules. The London, Edinburgh, and Dublin Philosophical Magazine and J Sci. 1905;10(57):318-40.
2. Brada M, Pijls-Johannesma M, De Ruysscher D. Current clinical evidence for proton therapy. Cancer J. 2009;15(4):319-24.
3. Newhauser WD, Zhang R. Phys Med Biol. 2015;60(8):R155-R209.
4. Barker DC, Lowe DM, Radhakrishna DG. An introduction to proton beam therapy. Br J Hosp Med (Lond). 2019;80(10):574-8.
5. Paganetti H. Range uncertainties in proton therapy and the role of Monte Carlo simulations. Phys Med Biol. 2012;57(11):R99-117.
6. Yang M, Zhu XR, Park PC, Titt U, Mohan R, Virshup G, et al. Comprehensive analysis of proton range uncertainties related to patient stopping-power-ratio estimation using the stoichiometric calibration. Phys Med Biol. 2012;57(13):4095-115.
7. Lomax AJ. Intensity modulated proton therapy and its sensitivity to treatment uncertainties 1: the potential effects of calculational uncertainties. Phys Med Biol. 2008;53(4):1027-42.
8. Zhu X, Fakhri GE. Proton therapy verification with PET imaging.

Theranostics. 2013;3(10):731-40.

9. Enghardt W, Debus J, Haberer T, Hasch BG, Hinz R, Jakel O, et al. Positron emission tomography for quality assurance of cancer therapy with light ion beams. Nucl Phys A. 1999;654(1, Suppl 1):1047c-50c.
10. Parodi K, Enghardt W. Potential application of PET in quality assurance of proton therapy. Phys Med Biol. 2000;45(11):N151-6.
11. Parodi K, Enghardt W, Haberer T. In-beam PET measurements of beta+ radioactivity induced by proton beams. Phys Med Biol. 2002;47(1):21-36.
12. Paans AMJ, Schippers JM. Proton therapy in combination with PET as monitor: A feasibility study. IEEE Trans Nucl Sci. 1993;40(4):1041-4.
13. Studenski MT, Xiao Y. Proton therapy dosimetry using positron emission tomography. World J Radiol. 2010;2(4):135-42.
14. Pawelke J, Enghardt W, Haberer T, Hasch BG, Hinz R, Kramer M, et al. In-beam PET imaging for the control of heavy-ion tumour therapy. IEEE Trans Nucl Sci. 1997;44(4):1492-8.
15. Enghardt W, Crespo P, Fiedler F, Hinz R, Parodi K, Pawelke J, et al. Charged hadron tumour therapy monitoring by means of PET. Nuclear Instruments and Methods in Physics Research Section A: Accelerators, Spectrometers, Detectors and Associated Equipment. 2004;525(1):284-8.
16. Iseki Y, Mizuno H, Futami Y, Tomitani T, Kanai T, Kanazawa M, et al. Positron camera for range verification of heavy-ion radiotherapy. Nuclear Instruments and Methods in Physics Research Section A: Accelerators, Spectrometers, Detectors and Associated Equipment. 2003;515:840-49.
17. Crespo P, Shakirin G, Fiedler F, Enghardt W, Wagner A. Direct time-of-flight for quantitative, real-time in-beam PET: A concept and feasibility study. Phys Med Biol. 2007;52(23):6795-811.
18. Parodi K, Paganetti H, Shih HA, Michaud S, Loeffler JS, DeLaney TF, et al. Patient study of in vivo verification of beam delivery and range, using positron emission tomography and computed tomography imaging after proton therapy. Int J Radiat Oncol Biol Phys. 2007;68(3):920-34.
19. Parodi K, Paganetti H, Cascio E, Flanz JB, Bonab AA, Alpert NM, et al. PET/CT imaging for treatment verification after proton therapy: A study with plastic phantoms and metallic implants. Med Phys. 2007;34(2):419-35.
20. Knopf A, Parodi K, Bortfeld T, Shih HA, Paganetti H. Systematic analysis of biological and physical limitations of proton beam range verification with offline PET/CT scans. Phys Med Biol. 2009;54(14):4477-95.
21. Knopf AC, Parodi K, Paganetti H, et al. Accuracy of proton beam range verification using post-treatment positron emission tomography/computed tomography as function of treatment site. Int J Radiat Oncol Biol Phys. 2011;79(1):297-304.
22. Phelps ME. PET: The merging of biology and imaging into molecular imaging. J Nucl Med. 2000;41(4):661-81.
23. Prasad R. Performance evaluation and development of quantitative procedures for high resolution preclinical PET imaging. 2013.
24. Fahey FH. Data acquisition in PET imaging. J Nucl Med Technol. 2002;30(2):39-49.
25. Tarantola G, Zito F, Gerundini P. PET instrumentation and reconstruction algorithms in whole-body applications. J Nucl Med. 2003;44(5):756-69.
26. Melcher CL. Scintillation crystals for PET. J Nucl Med. 2000;41(6):1051-5.
27. Spanoudaki V, Levin CS. Photo-detectors for Time of Flight Positron Emission Tomography (ToF-PET). Sensors (Basel, Switzerland). 2010;10(11):10484-505.
28. Casey ME, Nutt R. A multicrystal two dimensional BGO detector system for positron emission tomography. IEEE Trans Nucl Sci. 1986;33(1):460-63.
29. Cherry SR, Shao Y, Silverman RW. MicroPET: A high resolution PET scanner for imaging small animals. IEEE Trans Nucl Sci. 1997;44(3):1161-6.
30. Acilu PGd, Mendes PR, Cañadas M, Sarasola I, Cuerdo R, Romero L, et al. Evaluation of APD and SiPM matrices as sensors for monolithic PET detector blocks. 2011 IEEE Nucl Sci Symp Conf Rec.. 2011;2011.
31. Roncali E, Cherry SR. Application of silicon photomultipliers to positron emission tomography. Ann Biomed Eng. 2011;39(4):1358-77.
32. Badawi R. Introduction to PET Physics. University of Washington. 1999.
33. Llacer J. Positron emission medical measurements with accelerated radioactive ion beams. Nucl Sci Appl. 1988;3(2):111-31.
34. Enghardt W, Parodi K, Crespo P, Fiedler F, Pawelke J, Pönisch F. Dose quantification from in-beam positron emission tomography. Radiother Oncol. 2004;73 Suppl 2:S96-8.
35. Vecchio S, Attanasi F, Belcari N, Camarda M, Cirrone GAP, Cuttone G, et al. A PET prototype for in- beam monitoring of proton therapy. 2007;56.
36. Miyatake A, Nishio T, Ogino T, Saijo N, Esumi H, Uesaka M. Measurement and verification of positron emitter nuclei generated at each treatment site by target nuclear fragment reactions in proton therapy. Med Phys. 2010;37(8):4445-55.
37. Ferrero V, Fiorina E, Morrocchi M, Pennazio F, Baroni G, Battistoni G, et al. Online proton therapy monitoring: Clinical test of a Silicon-photodetector-based in- beam PET. Sci Rep. 2018;8(1):4100.
38. Shakirin G, Braess H, Fiedler F, Kunath D, Laube K, Parodi K, et al. Implementation and workflow for PET monitoring of therapeutic ion irradiation: A comparison of in-beam, in-room, and off-line techniques. Phys Med Biol. 2011;56(5):1281-98.
39. Nishio T, Ogino T, Nomura K, Uchida H. Dose-volume delivery guided proton therapy using beam on-line PET system. Med Phys. 2006;33(11):4190-97.
40. Zhu X, España S, Daartz J, Liebsch N, Ouyang J, Paganetti H, et al. Monitoring proton radiation therapy with in-room PET imaging. Phys Med Biol. 2011;56(13):4041-57.
41. Nishio T, Sato T, Kitamura H, Murakami K, Ogino T. Distributions of beta+ decayed nuclei generated in the CH_2 and H_2O targets by the target nuclear fragment reaction using therapeutic MONO and SOBP proton beam. Med Phys. 2005;32(4):1070-82.
42. Parodi K, Ferrari A, Sommerer F, Paganetti H. Clinical CT- based calculations of dose and positron emitter distributions in proton therapy using the FLUKA Monte Carlo code. Phys Med Biol. 2007;52(12):3369-87.